Ionics (2018) 24:3915–3921
https://doi.org/10.1007/s11581-018-2695-z

ORIGINAL PAPER

A comparative study on electrocatalytic performance of PtAu/C and PtRu/C nanoparticles for methanol oxidation reaction

Guodong Xu[1]

Received: 28 July 2018 / Revised: 9 August 2018 / Accepted: 10 August 2018 / Published online: 24 August 2018
© Springer-Verlag GmbH Germany, part of Springer Nature 2018

Abstract

We present a comparative study on the electrocatalytic performance of PtRu/C and PtAu/C nanoparticles for methanol oxidation reaction. The PtRu/C nanoparticles are commercially available, while the PtAu/C nanoparticles were prepared using the conventional sodium borohydride reduction method. The particle size, surface morphology, and crystallinity of the two samples were characterized using transmission electron microscopy (TEM) and X-ray diffraction (XRD). The electrocatalytic activity for MOR and the long-term durability of the PtAu/C and PtRu/C were carefully investigated. The results showed that the PtAu/C exhibited much higher activity for MOR and improved long-term durability in comparison with the PtRu/C. The catalysts before and after accelerated potential cycling test (APCT) were characterized by X-ray photoelectron spectroscopy (XPS). It was found that Ru dissolved and escaped completely from the electrode meanwhile the majority of Au remained after APCT.

Keywords PtAu nanoparticle · Sodium borohydride reduction · Methanol oxidation · Direct methanol fuel cell

Introduction

Fuel cells have been considered to be one of the most promising energy conversion devices for a wide variety of applications, most prominently electric vehicles [1]. Direct methanol fuel cells (DMFCs), as one class of fuel cells, have been intensely studied due to the obvious advantages of methanol with high energy density, low cost, abundance, renewability, and easy storage at near ambient conditions [2–4]. Currently, platinum is the most effective catalyst for methanol oxidation reaction (MOR) [5]. However, the intermediate species, CO, produced upon the indirect dehydrogenation of methanol was found to be adsorbed strongly on surfaces of pure platinum, leading to catastrophic catalyst poisoning and poor activity towards MOR. In the past decades, significant efforts have been made to develop low-cost, effective catalysts that are resistant against catalyst poisoning. It was demonstrated that the most effective technique is to modify platinum nanoparticles with foreign metals with adequate sizes and preferential shapes using metal oxides support [6–10].

The idea of introducing foreign metals into Pt catalysts has led rapid development of binary or ternary catalysts with enhanced electrocatalytic activities for MOR. In this context, the most effective catalyst for MOR was found to be Pt-Ru alloys [11–14]. To account for the enhanced electrocatalytic activity of PtRu for MOR, a bifunctional mechanism and electronic effect were proposed [15, 16]. It has been a consensus that Ru could promote water dissociation to provide active OH_{ads} for removal of CO_{ads} in the proximity of Pt atoms [11–17]. In addition, introduction of Ru atoms could also alter the electronic structures of the neighboring Pt atoms and weaken the adsorption strength of the intermediates on Pt surfaces, which facilitates intermediate removal.

Unfortunately, the instability of Ru in acidic media leads to a rapid decrease of activity for MOR during long-term operation [18–21]. To circumvent this issue and maintain high electrocatalytic activity for MOR, alternative catalysts via alloying Pt with other noble metals have been proposed [5, 6, 22, 23]. Among them, Au is an interesting one since

Electronic supplementary material The online version of this article (https://doi.org/10.1007/s11581-018-2695-z) contains supplementary material, which is available to authorized users.

✉ Guodong Xu
xuguodong003@gmail.com

[1] School of Chemistry and Environmental Engineering, Yancheng Teachers University, No. 2, Xiwang Avenue, Yancheng 224007, Jiangsu Province, China

it is inactive in a bulk state but highly catalytically active at nanoscale [24–27]. Gold nanoparticles have been found to be effective catalysts for CO oxidation at modest temperatures [28–31]. Furthermore, alloying with Au changes the electronic structure of Pt catalysts, lowering the adsorption energy of CO on catalyst surfaces. In addition, with an appropriate adjustment of synthetic procedure and metal ratio between Pt and Au, the obtained PtAu catalyst may exhibit the targeted electrocatalytic activity towards MOR [32–34]. As a consequence, PtAu bimetallic nanoparticles may serve as a promising anode catalyst for MOR.

In this paper, we report a simple and effective method to prepare a carbon-supported PtAu nanocatalyst using the conventional borohydride reduction method with trisodium citrate as the stabilizer agent. The loading level of Pt and Au was controlled to be 40 wt% and 20 wt% of the synthesized catalyst, respectively, in order to make an intuitive comparison with the commercial PtRu/C (Pt 40 wt% and Ru 20 wt%). At the same time, the molar ratio of Pt:Au was set to be around 2:1, which enables a high electrocatalytic activity for MOR. A higher proportion of Au in the alloy, such as 1:1, was found to dramatically reduce the electrocatalytic activity [26, 27, 32–34]. The synthesized PtAu/C exhibits better durability than the commercial PtRu/C catalysts from the results of an accelerated potential cycling test (APCT) [27, 35]. Furthermore, cyclic voltammograms of methanol oxidation suggest that PtAu/C possesses much higher mass activity for MOR than what was observed for commercial PtRu/C in a half-cell reaction.

Experimental

Materials

Commercially available PtRu/C (Pt 40 wt%, Ru 20 wt%, John Matthey), Pt/C (Pt 20 wt%, John Matthey), carbon paper (MGL190), and Nafion-117 (Dupont) were purchased from Alfa. The carbon paper was soaked in a PTFE (60 wt%) solution for 24 h followed by calcination at 350 °C for 2 h. Chloroplatinic acid and chloroauric acid were purchased from Shanxi Kaida Chemical Company. Vulcan XC-72 carbon black was ordered from Cabot. Five weight percent of a Nafion solution was obtained from Dupont. All chemicals were of analytical grade.

Catalyst preparation

The carbon-supported PtAu nanoparticles were prepared using the sodium borohydride reduction method as previously reported [29]. Generally, the required amounts of chloroplatinic acid, chloroauric acid, Vulcan XC-72 carbon powder, and trisodium citrate were dispersed in water via sonication. After the pH was adjusted to 9–10 using 6 M sodium hydroxide solution, an excess amount of sodium borohydride methanol solution was added dropwise. Subsequently, the mixture was kept stirring for another 12 h followed by filtration and rinse with a large amount of water. Finally, the carbon-supported platinum-gold (PtAu/C) was collected by drying in an oven at 80 °C for 3 h. The metal loading of Pt and Au was controlled to be 40 wt% and 20 wt%, respectively.

Fabrication of the working electrode for half-cell measurement

The catalyst ink was prepared via dispersing 4 mg of catalyst in a 1-mL mixture of ultrapure water, isopropanol, and 5 wt% Nafion solution. Then, 5 μL of ink was cast on a glassy carbon electrode (GCE) with 3-mm diameter.

Physical characterizations

The metal loading in the synthesized sample was evaluated via thermal gravimetric analysis in air. Powder X-ray diffraction (XRD) patterns of the synthesized PtAu/C and the commercial PtRu/C were obtained on D8-FOCUS, Bruker. The particle size and the surface morphology of the two samples were examined using high-resolution transmission electron microscope (HR-TEM) Tecnai G2 F 30. The X-ray photoelectron spectroscopy (XPS) measurements of the catalysts were carried out with a Physical Electronics PHI 5600 multi-technique system.

Electrochemical characterizations

The electrochemical measurements were recorded on a CHI 760E electrochemical workstation (CH Instrument). A conventional three-electrode cell was employed with a GCE as the working electrode, a platinum gauze electrode as the counter electrode, and a saturated calomel electrode (SCE) as the reference electrode, respectively.

All solutions used were deaerated by purging with ultrapure nitrogen gas for 20 min prior to measurements. The fabricated working electrode was kept cycling in a 0.5 M H_2SO_4 solution to provide reproducible cyclic voltammetry. All potentials were referenced to SCE unless specified. All electrochemical measurements were conducted at 25 °C.

The electrochemical surface area measurements

The cyclic voltammograms were conducted in a 0.5 M H_2SO_4 solution within the potential range of − 0.241 to 0.959 V at the scan rate of 50 mV s^{-1}. The electrochemical surface area (ECSA) of platinum of the synthesized PtAu/C and the commercial PtRu/C were calculated based on the coulombic

charges associated with hydrogen adsorption and desorption in the hydrogen region (− 0.241~0.1 V) after deducting the double-layer charging current [9, 27].

$$\mathrm{ECSA} = \frac{Q_{\mathrm{H}}}{0.21 \times M_{\mathrm{Pt}}}$$

where Q_{H} (mC) is the charge due to hydrogen adsorption/desorption in the hydrogen region of the CVs, 0.21 mC cm^{-2} is the electrical charge associated with the monolayer adsorption of hydrogen on Pt, and M_{Pt} is the loading of Pt metal on the working electrode.

Electrochemical CO stripping

The potential of the working electrode was initially held at − 0.14 V for 20 min with CO purging to enable complete adsorption on the electrode. Subsequently, the excess CO in the electrolyte was removed by purging nitrogen for 30 min. Finally, a cyclic voltammetry of CO stripping was applied.

Methanol oxidation reaction

The electrocatalytic oxidation of methanol was carried out in a 0.5 M H_2SO_4 solution with various methanol concentrations (1 M, 2 M, and 4 M) within the potential from 0 to 0.959 V at the scan rate of 50 mV s^{-1}.

The accelerated potential cycling test

The stability of the anode catalyst was evaluated via a square wave between 0.37 to 0.73 V at the scan rate of 120 mV s^{-1} in 0.5 M H_2SO_4. ECSA measurements were conducted for every 600 APCT cycles.

Results and discussion

The procedure of synthesizing PtAu/C nanoparticles was described in the "Experimental" section. The metal loading of the synthesized compound was evaluated by thermal gravimetric analysis in air as depicted in Fig. S1 (supporting information). The overall loading of Pt and Au is 57 wt%, quite close to the stoichiometric value, indicating successful reduction of the Pt and Au precursors. In comparison, the commercial PtRu/C was also evaluated by TGA in Fig. S2. The 67 wt% residue is attributed to Pt and RuO_2, correlating with the 40 wt% Pt and 20 wt% Ru in the commercial catalyst.

The particle size and the morphology of the synthesized PtAu/C nanocatalyst and the commercial PtRu/C nanoparticles were determined by TEM (Fig. 1). It is obvious that aggregation occurred during the PtAu/C nanoparticle synthesis using the conventional sodium borohydride reduction method with trisodium citrate as the stabilizer, which is different from using the functionalized carbon nanotubes as support as reported in the previous study [32]. This is probably attributed to the weak interaction between carbon black and the metal precursors in the synthesis process. Unlike the PtAu/C nanoparticles, the PtRu nanoparticles were well dispersed in the commercial PtRu/C sample with the average diameter around 3 nm.

The crystallinity of bimetallic PtAu nanostructure on carbon was characterized by PXRD. In addition, the XRD patterns of the commercial PtRu/C sample were also collected for comparison (Fig. 2). The prominent (111) peaks were observed for both catalysts, indicating a face-centered cubic

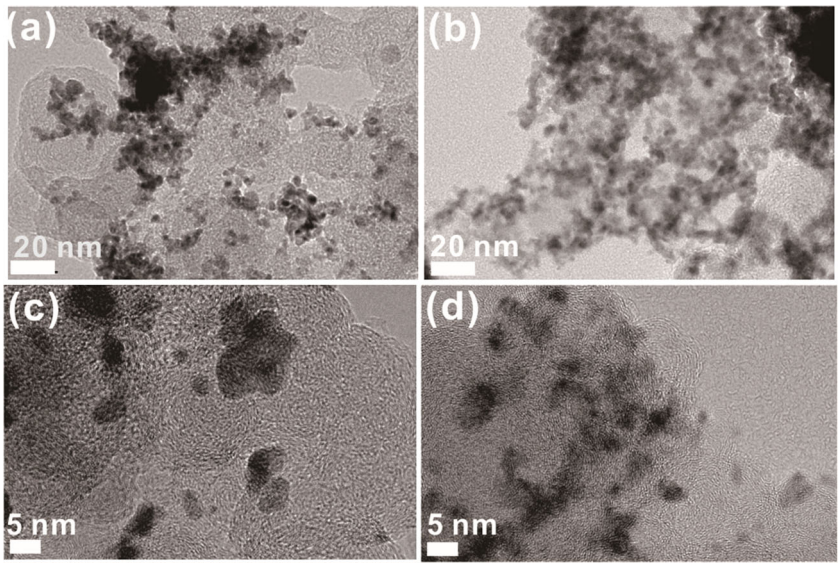

Fig. 1 The TEM and HR TEM images of PtAu/C (**a**), PtRu/C (**b**), PtAu (**c**), and PtRu (**d**) nanoparticles

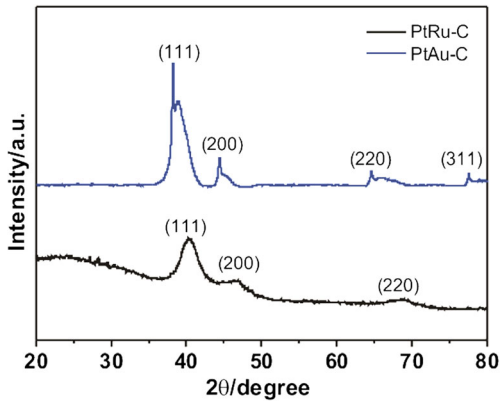

Fig. 2 The XRD patterns of PtAu/C (blue line) and PtRu/C (black line)

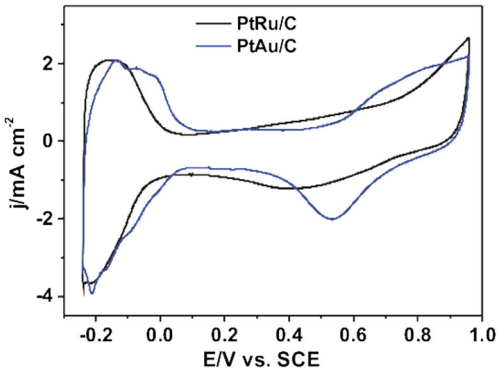

Fig. 3 The cyclic voltammograms of the commercial PtRu/C catalyst (black line) and the synthesized PtAu/C (blue line) catalyst in a N_2-saturated 0.5 M H_2SO_4 solution. The scanning rate is 50 mV s^{-1}

structure. Two sets of (111) peaks were found in the diffraction patterns of PtAu/C, suggesting that phase separation occurs in this sample. The (111) peak values are listed in Table 1. The diffraction at 38.21° in PtAu/C correlates well with the (111) peak of Au metal, suggesting that aggregation of the Au nanoparticles takes place. The diffraction peak at 38.86° in PtAu/C indicates the existence of a PtAu alloy. In contrast, Pt and Ru are well alloyed in the PtRu/C sample with the (111) diffraction peak at 40.43°.

The cyclic voltamograms of the PtAu/C nanoparticles and the commercial PtRu/C sample were performed in deaerated 0.5 M H_2SO_4. Figure 3 shows the Pt oxidation, Pt oxide reduction and the characteristic hydrogen adsorption/desorption peaks for both catalysts. The platinum oxide reduction peak in the PtAu/C nanoparticles is larger than that of the commercial PtRu/C catalyst, indicating a smaller degree of alloying for PtAu/C, which is consistent with the results of PXRD. The current associated with the characteristic hydrogen region (adsorption and desorption) of the PtAu/C catalyst is similar to that of the commercial PtRu/C sample, suggesting that the two compounds have similar electrochemical surface areas. The estimated values of ECSAs of PtAu/C and PtRu/C are 28.8 m^2 $g^{-1}{}_{Pt}$ and 30.7 m^2 $g^{-1}{}_{Pt}$, respectively. A lower ECSA value of PtAu/C is attributed to the aggregated nanoparticles as found in the TEM image.

The electrocatalytic activity for MOR of the two catalysts was investigated in 0.5 M H_2SO_4 with various methanol concentrations and the results are depicted in Fig. 4a, b. The current density was normalized by the mass specific activity of Pt. Two well-defined anodic peaks are observed.

Table 1 The values of the diffraction peaks of PtAu/C and PtRu/C

Catalyst	Peak (111)	2θ value (°)
PtAu/C	Au	38.21
	PtAu	38.86
PtRu/C	PtRu	40.43

The forward oxidation peak at around 0.65 V corresponds to dehydrogenation of methanol, which usually involves both direct and indirect dehydrogenation pathways [36]:

$$\text{Direct pathway: } \mathrm{Pt}(CH_3OH)_{ads} + H_2O \rightarrow CO_2 + 6H^+ + 6e^-$$

$$\text{Indirect pathway: } \mathrm{Pt}(CH_3OH)_{ads} \rightarrow Pt(CO)_{ads} + 6H^+ + 6e^-$$

Along with the indirect pathway of methanol oxidation, intermediates such as CO and CHO are formed and may be adsorbed strongly on the electrode surface. In the backward scan, these intermediates are oxidized and platinum oxides are reduced simultaneously at around 0.45 V. The values of the forward scan peak current densities in various methanol concentrations of PtAu/C and PtRu/C are shown in Fig. 4c. The forward mass activities of PtRu/C are 36.2, 120.8, and 195.4 mA $mg^{-1}{}_{Pt}$ for 1 M, 2 M, and 4 M of methanol solutions, respectively. The forward mass activities of PtAu/C are 105.9, 216.1, and 332.1 mA $mg^{-1}{}_{Pt}$ for 1 M, 2 M, and 4 M of methanol solutions, respectively, about 3 times, 2 times, and 1.5 times larger than the corresponding values of PtRu/C. Remarkably, the PtAu/C catalyst exhibits much higher electrocatalytic activity for MOR than the PtRu/C catalyst which has long been considered as the most efficient catalyst for MOR [11, 12]. The high electrocatalytic activity of PtAu/C for MOR is probably attributed to the oxidation capability of Au for both methanol and CO at nanoscale [24, 30, 37]. Another possible reason is that the low-alloyed PtAu nanoparticles indicated by XRD results may possess a structure similar to core-shell structure with a Pt-rich shell and a gold-rich core as a result of a faster deposition of Au than Pt in excess sodium borohydride solution, because of the large redox potential difference between the two redox couples (E ($PtCl_6^{2-}$/Pt(0) = 0.717 V; E ($AuCl^{4-}$/Au(0) = 1.002 V). As a consequence, the surface area of Pt is more exposed in PtAu/C compared to that of PtRu/C, leading to a high catalytic activity to MOR. Likewise, the backward mass activities of PtAu/C are again much larger than the values of PtRu/C. The I_f/I_b values of

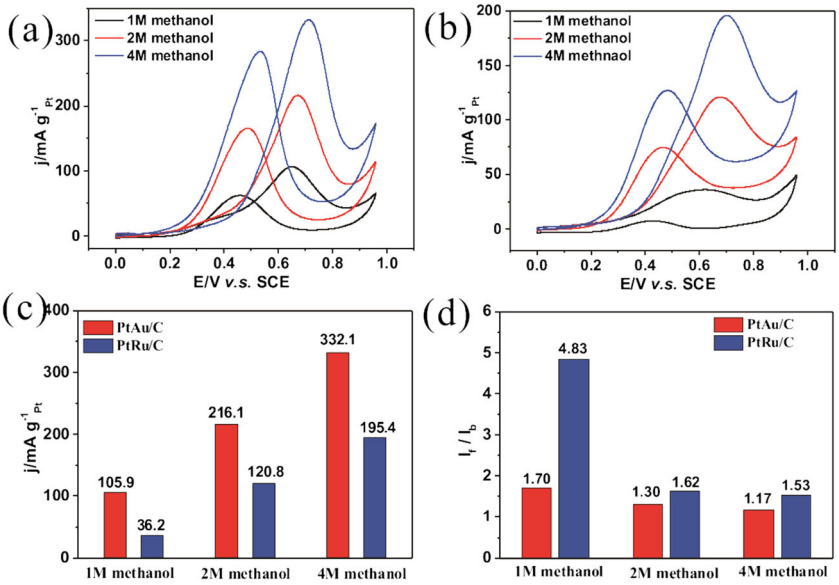

Fig. 4 The cyclic voltammograms of methanol electrooxidation of PtAu/C (**a**) and PtRu/C (**b**) in a solution of 0.5 M H_2SO_4 with various methanol concentrations. (**c**) The specific activity for PtAu/C and PtRu/C in 0.5 M H_2SO_4 with 1 M, 2 M, and 4 M methanol. (**d**) The ratio of the forward anodic peak current density (I_f) to the reverse anodic peak current density (I_b). The scanning rate is 50 mV s^{-1}

PtAu/C and PtRu/C in different methanol concentrations are depicted in Fig. 4d. Apparently, the I_f/I_b value of PtRu/C is much larger than that of PtAu/C in 1 M methanol, attributed to the excellent bifunctional mechanism of Ru [13]. However, the PtAu/C exhibits comparable performance of CO tolerance in comparison with the PtRu/C when using 2 M or higher methanol concentrations.

In addition to the high electroactivity for MOR, the PtAu/C displays good durability because of the great stability of gold. The durability of these two catalysts was evaluated using accelerated potential cycle test (APCT). The cyclic voltammograms of the two catalysts before and after APCT are depicted in Fig. 5a, b. The current density decreases rapidly with cycle numbers in the case of the PtRu/C. And the final current density of the PtRu/C is obviously smaller than that of the PtAu/C. The normalized ECSAs of Pt particles of two compounds are shown in Fig. 5c, d, respectively. From Fig. 5d, the ECSA of PtRu/C is reduced by 49% after APCT. However, the ECSA of PtAu/C remains at 70% after APCT as shown in Fig. 5c, suggesting that PtAu/C has a better long-term stability.

The poor durability of the PtRu/C is probably due to the easy dissolution of Ru in acidic media. Meanwhile, the high resistance to dissolution in acidic media of Au leads to an improved stability. To confirm our expectation, the PtAu/C and the PtRu/C before and after APCT were characterized

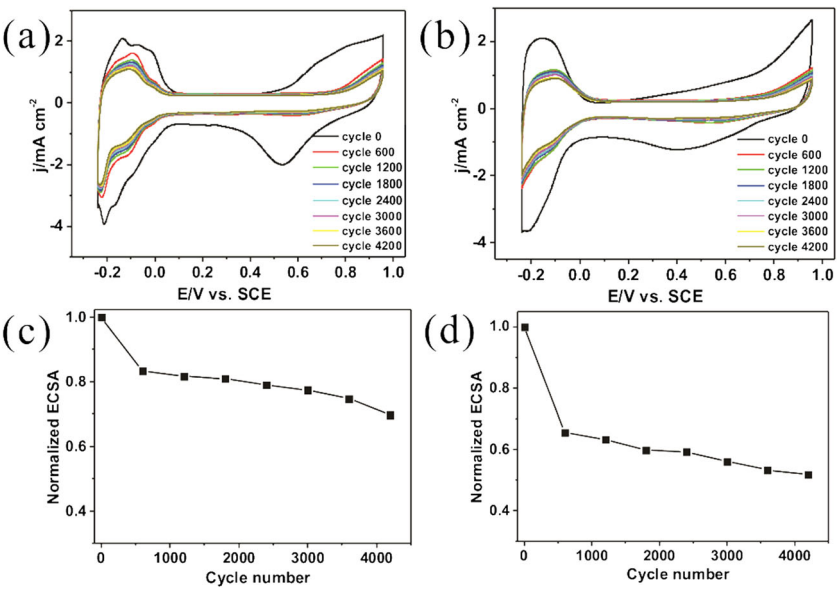

Fig. 5 CV in 0.5 M H_2SO_4 for PtAu/C (**a**) and CV in 0.5 M H_2SO_4 for PtRu/C (**b**) during the APCT. The normalized ECSAs and the cycle numbers for PtAu/C (**c**) and PtRu/C (**d**) during the APCT. The scanning rate is 50 mV s^{-1}

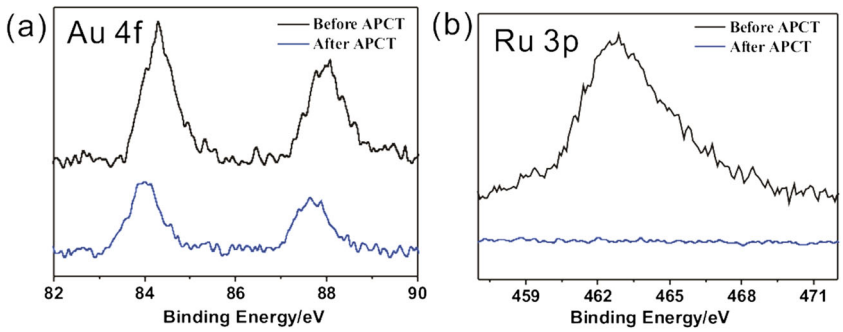

Fig. 6 Regional XPS of (**a**) Au 4f and (**b**) Ru 3p before and after APCT of the PtAu/C and the PtRu/C, respectively

with X-ray photoelectron spectroscopy (XPS). Figure 6a displays the Au 4f region in the PtAu/C before and after APCT. Prominent peaks attributed to Au 4f were observed after APCT with a small negative shift, suggesting that Au was not oxidized after the durability test. The relatively lower peaks of Au 4f after APCT are probably attributed to the small amount of sample used because the sample after APCT was peeled off from a 3-mm GCE. Figure 6b shows the Ru 3p instead of the Ru 3d because the latter always with the C 1s spectrum. It was found that the peak associated with Ru 3p diminished after APCT, suggesting that the Ru dissolved and escaped from the electrode during the durability test. These results are in agreement with our expectation.

CO tolerance is an important parameter for anode catalyst towards MOR. To evaluate the CO tolerance capability between PtAu/C and PtRu/C, the CO stripping voltammetry was performed in 0.5 M H_2SO_4. The CO stripping curves of the two compounds are depicted in Fig. S3. The peak potentials for CO oxidation on PtAu/C and on PtRu/C are 0.57 V and 0.41 V vs. SCE, respectively. The smaller positive potential towards CO oxidation of the PtRu/C catalyst confirms the bifunctional mechanism of Ru and demonstrates the higher CO tolerance of the PtRu/C catalyst.

Conclusion

We have synthesized a highly effective electrocatalyst of PtAu/C nanoparticles using the conventional sodium borohydride reduction method. The successful reduction of Pt and Au precursors was confirmed by thermal gravimetric analysis. Phase separation (Au and PtAu) in the sample was identified from the XRD spectrum during the synthesis procedure due to the weak interaction between the carbon support and the metal precursors. The synthesized PtAu/C nanocatalyst exhibits an ECSA of 28.8 $m^2\ g^{-1}_{Pt}$ comparable to the value of the commercial PtRu/C sample (30.8 $m^2\ g^{-1}_{Pt}$). Remarkably, the PtAu/C catalyst also exhibits much higher electrocatalytic activity for MOR than the PtRu/C catalyst in the half-cell reaction. Furthermore, the PtAu/C catalyst displays significantly enhanced durability during APCT. The ECSA of PtAu/C remains at 70% after APCT, while the ECSA of PtRu/C is reduced to 51%. Further enhancement of the catalytic activity for the PtAu nanoparticles is envisaged through improvement of Pt and Au alloying degree via enhancing the interaction between support and noble metal precursors.

Funding information This study received support by the grants from the National Natural Science Foundation of China (Nos. 21233006 and 21473164) and a start-up grant from Yancheng Teachers University (72061871001C).

Compliance with ethical standards

Conflict of interest The author declares that he has no conflict of interest.

References

1. Schlapbach L, Zuttel A (2001) Hydrogen-storage materials for mobile applications. Nature 414:353–358
2. Ahmed M, Dincer I (2011) A review on methanol crossover in direct methanol fuel cells: challenges and achievements. Int J Energy Res 35:1213–1228
3. Hunt ST, Milina M, Alba-Rubio AC, Hendon CH, Dumesic JA, Román-Leshkov Y (2016) Self-assembly of noble metal monolayers on transition metal carbide nanoparticle catalysts. Science 352:974–978
4. Kamarudin SK, Achmad F, Daud WRW (2009) Overview on the application of direct methanol fuel cell (DMFC) for portable electronic devices. Int J Hydrog Energy 34:6902–6916
5. Kakati N, Maiti J, Lee SH, Jee SH, Viswanathan B, Yoon YS (2014) Anode catalysts for direct methanol fuel cells in acidic media: do we have any alternative for Pt or Pt–Ru? Chem Rev 114: 12397–12429
6. Yu X, Wang D, Peng Q, Li Y (2013) Pt M (M=Cu, Co, Ni, Fe) nanocrystals: from small nanoparticles to wormlike nanowires by oriented attachment. Chem Eur J 19:233–239
7. Zhao Y, Wang F, Tian J, Yang X, Zhan L (2010) Preparation of Pt/CeO_2/HCSs anode electrocatalysts for direct methanol fuel cells. Electrochim Acta 55:8998–9003
8. Qi J, Xin L, Zhang Z, Sun K, He H, Wang F, Chadderdon D, Qiu Y, Liang C, Li W (2013) Surface dealloyed PtCo nanoparticles supported on carbon nanotube: facile synthesis and promising application for anion exchange membrane direct crude glycerol fuel cell. Green Chem 15:1133

9. Jiang Z-Z, Wang Z-B, Chu Y-Y, Gu D-M, Yin G-P (2011) Ultrahigh stable carbon riveted Pt/TiO_2-C catalyst prepared by in situ carbonized glucose for PEMFC. Energy Environ Sci 4:728–735
10. Cui Z, Feng L, Liu C, Xing W (2011) Pt nanoparticles supported on WO_3/C hybrid materials and their electrocatalytic activity for methanol electro-oxidation. J Power Sources 196:2621–2626
11. Iwasita T, Hoster H, John-Anacker A, Lin WF, Vielstich W (2000) Methanol oxidation on PtRu electrodes. Influence of surface structure and Pt−Ru atom distribution. Langmuir 16:522–529
12. Guo JW, Zhao TS, Prabhuram J, Chen R, Wong CW (2005) Preparation and characterization of a PtRu/C nanocatalyst for direct methanol fuel cells. Electrochim Acta 51:754–763
13. Li L, Xing Y (2007) Pt−Ru nanoparticles supported on carbon nanotubes as methanol fuel cell catalysts. J Phys Chem C 111: 2803–2808
14. Zhou Y, Yang G, Pan H-B, Zhu C, Fu S, Shi Q, du D, Cheng X, Yang J, Wai CM, Lin Y (2015) Ultrasonic-assisted synthesis of carbon nanotube supported bimetallic Pt-Ru nanoparticles for effective methanol oxidation. J Mater Chem A 3:8459–8465
15. Davies JC, Hayden BE, Pegg DJ (2000) The modification of Pt(110) by ruthenium: CO adsorption and electro-oxidation. Surf Sci 467:118–130
16. Roth C, Benker N, Buhrmester T, Mazurek M, Loster M, Fuess H, Koningsberger DC, Ramaker DE (2005) Determination of O [H] and CO coverage and adsorption sites on PtRu electrodes in an operating PEM fuel cell. J Am Chem Soc 127:14607–14615
17. Ma L, Liu C, Liao J, Lu T, Xing W, Zhang J (2009) High activity PtRu/C catalysts synthesized by a modified impregnation method for methanol electro-oxidation. Electrochim Acta 54:7274–7279
18. Chung Y, Pak C, Park G-S, Jeon WS, Kim JR, Lee Y, Chang H, Seung D (2008) Understanding a degradation mechanism of direct methanol fuel cell using TOF-SIMS and XPS. J Phys Chem C 112: 313–318
19. Taniguchi A, Akita T, Yasuda K, Miyazaki Y (2004) Analysis of electrocatalyst degradation in PEMFC caused by cell reversal during fuel starvation. J Power Sources 130:42–49
20. Piela P, Eickes C, Brosha E, Garzon F, Zelenay P (2004) Ruthenium crossover in direct methanol fuel cell with Pt-Ru black anode. J Electrochem Soc 151:A2053
21. Gu Z, Li S, Xiong Z, Xu H, Gao F, Du Y (2018) Rapid synthesis of platinum-ruthenium bimetallic nanoparticles dispersed on carbon support as improved electrocatalysts for ethanol oxidation. J Colloid Interface Sci 521:111–118
22. Song P, Xu H, Wang J, Shiraishi Y, Du Y (2018) Construct 3D networked Au-Cu nanowires for enhanced plasmon-driven catalytic ethylene glycol oxidation through visible light irradiation. J Power Sources 399:59–65
23. Gao F, Xu H, Zhang Y, Wang J, Wang C, Du Y (2018) Facile construction of pompon-like PtAg alloy catalysts for enhanced ethylene glycol electrooxidation. Int J Hydrog Energy 43:9644–9651
24. Haruta M (2005) Catalysis: gold rush. Nature 437:1098–1099
25. Choi J-H, Park K-W, Park I-S, Kim K, Lee J-S, Sung Y-E (2006) A PtAu nanoparticle electrocatalyst for methanol electro-oxidation in direct methanol fuel cells. J Electrochem Soc 153:A1812
26. Y H, Zhang H, P W, Zhang H, Zhou B, Cai C (2011) Bimetallic Pt-Au nanocatalysts electrochemically deposited on graphene and their electrocatalytic characteristics towards oxygen reduction and methanol oxidation. Phys Chem Chem Phys 13:4083
27. Selvaganesh SV, Selvarani G, Sridhar P, Pitchumani S, Shukla AK (2011) Durable electrocatalytic-activity of Pt-Au/C cathode in PEMFCs. Phys Chem Chem Phys 13:12623–12634
28. Rodriguez P, Plana D, Fermin DJ, Koper MTM (2014) New insights into the catalytic activity of gold nanoparticles for CO oxidation in electrochemical media. J Catal 311:182–189
29. Rodriguez P, Kwon Y, Koper MTM (2012) The promoting effect of adsorbed carbon monoxide on the oxidation of alcohols on a gold catalyst. Nat Chem 4:177–182
30. Ide MS, Davis RJ (2014) The important role of hydroxyl on oxidation catalysis by gold nanoparticles. Acc Chem Res 47:825–833
31. Rolison DR (2003) Catalytic nanoarchitectures–the importance of nothing and the unimportance of periodicity. Science 299:1698–1701
32. Wang J, Yin G, Liu H, Li R, Flemming RL, Sun X (2009) Carbon nanotubes supported Pt–Au catalysts for methanol-tolerant oxygen reduction reaction: a comparison between Pt/Au and PtAu nanoparticles. J Power Sources 194:668–673
33. Selvarani G, Selvaganesh SV, Krishnamurthy S et al (2009) A methanol-tolerant carbon-supported Pt−Au alloy cathode catalyst for direct methanol fuel cells and its evaluation by DFT. J Phys Chem C 113:7461–7468
34. Xu JB, Zhao TS, Yang WW, Shen SY (2010) Effect of surface composition of Pt-Au alloy cathode catalyst on the performance of direct methanol fuel cells. Int J Hydrog Energy 35:8699–8706
35. Takenaka S, Miyamoto H, Utsunomiya Y, Matsune H, Kishida M (2014) Catalytic activity of highly durable Pt/CNT catalysts covered with hydrophobic silica layers for the oxygen reduction reaction in PEFCs. J Phys Chem C 118:774–783
36. Zhao X, Yin M, Ma L, Liang L, Liu C, Liao J, Lu T, Xing W (2011) Recent advances in catalysts for direct methanol fuel cells. Energy Environ Sci 4:2736
37. Peng S, Lee Y, Wang C, Yin H, Dai S, Sun S (2008) A facile synthesis of monodisperse Au nanoparticles and their catalysis of CO oxidation. Nano Res 1:229–234